Journal of Atmospheric and Solar-Terrestrial Physics 102 (2013) 99–104

Contents lists available at SciVerse ScienceDirect

Journal of Atmospheric and Solar-Terrestrial Physics

journal homepage: www.elsevier.com/locate/jastp

Interannual variations of MLS carbon monoxide induced by solar cycle

Jae N. Lee [a,*], Dong L. Wu [b], Alexander Ruzmaikin [c]

[a] Joint Center for Earth Systems Technology, University of Maryland, Baltimore County, Baltimore, MD, USA
[b] NASA Goddard Space Flight Center, Greenbelt, MD, USA
[c] Jet Propulsion Laboratory, California Institute of Technology, Pasadena, CA, USA

ARTICLE INFO

Article history:
Received 18 October 2012
Received in revised form
29 April 2013
Accepted 17 May 2013
Available online 25 May 2013

Keywords:
Carbon monoxide
Total solar irradiance
Middle atmosphere
Microwave Limb Sounder

ABSTRACT

More than eight years (2004–2012) of carbon monoxide (CO) measurements from the Aura Microwave Limb Sounder (MLS) are analyzed. The mesospheric CO, largely produced by the carbon dioxide (CO_2) photolysis in the lower thermosphere, is sensitive to the solar irradiance variability. The long-term variation of observed mesospheric MLS CO concentrations at high latitudes is likely driven by the solar-cycle modulated UV forcing. Despite of different CO abundances in the southern and northern hemispheric winter, the solar-cycle dependence appears to be similar. This solar signal is further carried down to the lower altitudes by the dynamical descent in the winter polar vortex. Aura MLS CO is compared with the Solar Radiation and Climate Experiment (SORCE) total solar irradiance (TSI) and also with the spectral irradiance in the far ultraviolet (FUV) region from the SORCE Solar-Stellar Irradiance Comparison Experiment (SOLSTICE). Significant positive correlation (up to 0.6) is found between CO and FUV/TSI in a large part of the upper atmosphere. The distribution of this positive correlation in the mesosphere is consistent with the expectation of CO changes induced by the solar irradiance variations.

1. Introduction

A long photochemical lifetime and strong vertical and horizontal gradients make carbon monoxide (CO) a good tracer for studying dynamics of the middle atmosphere (Allen et al., 2000; Lee et al., 2011). Aura Microwave Limb Sounder (MLS) CO shows a CO volume mixing ratio (VMR) exceeding 20 ppmv (parts per million by volume) in the winter polar upper mesosphere. Generally speaking, the CO mixing ratio decreases with height in the lower stratosphere, reaching a minimum around 30 hPa, then increases with height up to the thermosphere due to its high altitude source. While some CO is produced by the oxidation of methane in the stratosphere, most of the stratospheric and mesospheric CO is created by photolysis of carbon dioxide (CO_2) in the upper mesosphere and thermosphere and transported down to the lower mesosphere and stratosphere (Solomon et al., 1985; Allen et al., 1999):

$$CO_2 + h\nu \rightarrow CO + O \quad (1)$$

As seen from the CO_2 absorption cross-section, the photodissociation takes place most effectively at the solar Lyman α (121.6 nm) and Schumann–Runge band (175 nm–200 nm) radiation, which is effective only at high altitudes (Solomon et al., 1985; Brasseur and Solomon, 2005; Minschwaner et al., 2010; and references therein). The photolysis intensity varies with the solar irradiance, especially with the contributions from Lyman α in the upper middle atmosphere (mesosphere and lower thermosphere) and those from the Schumann–Runge bands in the mesosphere and stratosphere.

The CO_2 photodissociation rate evaluated with MLS and Atmospheric Chemistry Experiment-Fourier Transform Spectrometer (ACE-FTS) measurements show that it maximizes near 145 nm in the thermosphere (Minschwaner et al., 2010). The dominant contribution to photo-dissociation occurs at wavelengths greater than 175 nm where the O_2 Schumann–Runge bands control the atmospheric opacity. Solar ultraviolet irradiances were taken from the Solar Ultraviolet Spectral Irradiance Monitor (SUSIM) measurement in their photo-dissociation frequency calculation.

Laboratory measurements of the absorption cross sections of CO_2 have been made in the region 117 -200 nm (Yoshino et al., 1996; Parkinson et al., 2003). These measurements show that the absorption cross sections of CO_2 is maximum near 135–145 nm. CO_2 photolysis is a function of solar UV spectral irradiance, CO_2 cross section, and atmospheric opacity, so that the relevant wavelengths depend on altitude.

A major chemical loss of CO above ~100 km is due to a three-body recombination with atomic oxygen:

$$CO + O + M \rightarrow CO_2 + M \quad (2)$$

However, the photochemical time of the above reaction is much slower than transport at these altitudes. In the upper stratosphere and mesosphere, CO is also produced by methane oxidation (not

* Corresponding author. Tel.: +1 301 614 6189; fax: +1 301 614 6307.
E-mail address: jae.n.lee@nasa.gov (J.N. Lee).

1364-6826/$ - see front matter © 2013 Elsevier Ltd. All rights reserved.
http://dx.doi.org/10.1016/j.jastp.2013.05.012

shown) and rapidly destroyed by the OH oxidation, i.e.,

$$CO + OH \rightarrow CO_2 + H \quad (3)$$

This reaction occurs mostly during the day, since upper-atmospheric OH is produced from photolysis reactions (e.g., with H_2O).

Chemical loss of the thermospheric CO is negligible due to low amount of OH. It gives CO a long lifetime to be transported down to the mesosphere. In the polar night, mesospheric CO is conserved due to lack of OH. Therefore, CO VMR has a small diurnal variation and can be used as a tracer of atmospheric dynamics in both day and night, particularly in the wintertime polar dynamics.

The CO lifetime is long enough to maintain the anomalous distribution of CO inside the vortex throughout the descent from the mesosphere to the lower stratosphere over 30 days in the polar stratosphere and mesosphere during winter (Minschwaner et al., 2010; Lee et al., 2011). It has a relatively shorter lifetime (about 10 days) at the low and mid-latitudes in the mid to upper stratosphere, which helps to remove CO quickly once it is mixed out of the vortex.

In addition to the photochemical sources, ionization by energetic particles, primarily by electrons with energies of ~1–6 MeV in the auroral regions, is another source of mesospheric CO, as suggested by Marsh (2011). Statistically significant tracer composition changes with large solar photon events (SPEs) are shown with the Whole Atmosphere Community Climate Model (WACCM3) and various satellite instrument measurements (Jackman et al., 2008, 2009, 2011), but significant CO changes with SPE were not reported yet.

The unique CO lifetime and photolysis lead to a large vertical gradient with VMR values from ppmv in the mesosphere to ppbv (parts per billion per volume) in the low stratosphere. The descending air in the wintertime polar vortex brings CO further down to the lower stratosphere, producing strong hemispheric asymmetry in its concentration in the middle atmosphere (Solomon et al., 1985).

The seasonal climatology of zonal mean CO abundance shows maxima during the winter in the high-latitude region (Filipiak et al., 2005; Jin et al., 2009), which is a manifestation of the summer-to-winter meridional circulation at these altitudes and the descending air motion near the winter pole. Dynamical perturbations from planetary and gravity wave activities also contribute to large CO variability at the extra-tropics in the middle atmosphere (Allen et al., 1999). CO variances in middle atmosphere tropics are largely affected by QBO and solar influences are relatively weak in that region.

Understanding mesospheric CO variability requires accurate measurements of solar spectral irradiance in order to quantify the CO photolysis input modulated by the solar cycle. Recent Solar Radiation and Climate Experiment (SORCE) observations of solar irradiance from the space (Rottman, 2005; Pilewskie et al., 2005) enable us to investigate the response of the photolysis driven CO, which can be sensitive to the solar 11-year and 27-day variability, and to the SPEs.

The SORCE Total Irradiance Monitor (TIM) observations reveal that the averaged total solar irradiance (TSI) is ~1360.8 W/m^2 during the 2008 solar minimum, ~5 W/m^2 lower than the previously reported values (Kopp and Lean, 2011). The lower TSI values are due to the advanced design of the TIM in which the scattered light, a primary cause of the higher irradiance values measured by the earlier generation of solar radiometers, is precluded by the forward replacement of the defining aperture relative to the view-limiting aperture. TIM observations also indicate that the TSI into the Earth's atmosphere changes by about ~0.1% from solar minimum to solar maximum.

The SORCE Solar-Stellar Irradiance Comparison Experiment (SOLSTICE) measures the solar spectral irradiance in ultraviolet (UV) from 115 to 320 nm with a resolution of 0.1 nm, an absolute accuracy of better than 5%, and a relative accuracy of 0.5% per year (McClintock et al., 2005a, 2005b; Snow et al., 2005). The SOLSTICE measurements are made using a pair of identical spectrometers, SOLSTICE A and SOLSTICE B. Each spectrometer independently makes ultraviolet spectral measurements in two intervals: far ultraviolet (FUV) in 115–180 nm and mid ultraviolet (MUV) in180–320 nm.

Spectral measurement of solar radiation from SORCE Spectral Irradiance Monitor (SIM) shows that solar irradiance changes over 11-year cycle are wavelength dependent (Harder et al., 2009). These findings are incorporated into the Sun-climate inter connection studies (Haigh et al., 2010; Merkel et al., 2011; Li et al., 2012; Swartz et al., 2012) since different regions of the Earth's atmosphere respond differently to each part of the solar irradiance spectrum.

The Aura MLS data, which cover the solar minimum period between the cycles 23 and 24, contain useful insights on the solar-driven chemistry and dynamics of the middle atmosphere. The 27-day variations in MLS stratospheric ozone and temperature were investigated in comparison with SORCE UV radiation by Ruzmaikin et al. (2007). In this study we focus on interannual variations of the mesospheric CO observed by MLS and analyze the data in comparison with TSI measured by SORCE TIM. We find a good correlation between the MLS mesospheric CO and the solar irradiance variations, suggesting the long-term MLS CO variation in the mesosphere is likely tracing the 11-year solar cycle.

2. Data and Methods

We use the version 2.2 of the MLS data for the daily CO, gridded separately for day and night at 29 pressure levels from the upper troposphere (316 hPa) to the mesopause (~0.005 hPa). The daily CO fields are mapped onto a 4° (latitude) × 8° (longitude) grid for daytime (ascending) and nighttime (descending) orbits. Because Aura MLS sampling does not cover the regions poleward of 82° latitude, we use the observations in latitude bins between 82°N and 82°S during the winter months (December for Northern Hemisphere (NH); July for Southern Hemisphere (SH). The typical single-profile precision of MLS V2.2 CO varies from 0.02 ppmv at 100 hPa, 0.2 ppmv at 1 hPa, to 11 ppmv at 0.002 hPa, with vertical resolution of 4, 3, and 9 km, respectively (Pumphrey et al., 2007). MLS has a good vertical and horizontal resolution (9 km × 200 km) and single profile precision of 11 ppmv in the upper mesosphere.

As shown in the zonal mean CO in section 3, there is a large meridional gradient in its volume mixing ratio. This gradient, evident in MLS radiance measurements as well, is not affected by the universal initial guess used in the retrieval algorithm. Random errors in MLS CO must be greatly reduced in the monthly mean data. However, there is a significant day to day variability in the monthly zonal mean CO which is included in the standard deviation as shown in Fig. 1.

The TSI data from the TIM is used in this study as a proxy of solar irradiance variation over solar cycle. The SORCE TIM TSI data have 3 times higher accuracy (0.035%) than prior TSI measurements and with a long term stability of 0.001% per year (Kopp and Lawrence, 2005; Kopp et al., 2005). The FUV data from SORCE SOLSTICE is also used to show the solar cycle in CO concentration. The SORCE SOLSTICE instrument has spectral coverage in FUV (115–180 nm) and MUV (180–320 nm), but we only used far ultraviolet (FUV) integrated over 120 nm–160 nm band to avoid the discontinuities in the FUV and MUV spectrum near 180 nm region.

To study the CO dependence on the solar-cycle forcing, we search for correlations between the MLS CO and SORCE TSI/FUV

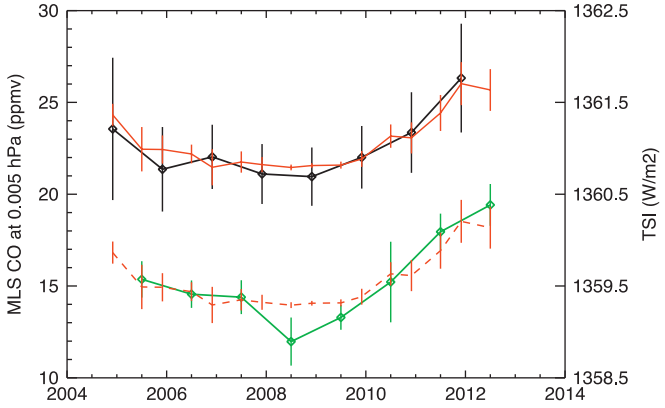

Fig. 1. Monthly mean MLS CO VMR for December at 82°N (black) and July at 82°S (green) at 0.005 hPa. Red curve is the monthly SORCE TSI with standard deviation. Dotted red curve is the same TSI values but shifted down by 1.5 W/m^2 for illustrating the correlation with the CO change in the SH. In both CO and TSI, the standard deviation is calculated from daily zonal mean values.

using monthly averaged data during December 2004–July 2012. We also perform the correlation study with the daily data for the same period to analyze the solar signal and other variations in CO at shorter periods. Due to the strong seasonal dependence of the mesospheric CO composition, we extract the solar-cycle signal separately for the boreal winter (December) and austral winter (July) seasons.

We limit the time of our analysis within the winter season when the solar signal in CO is significant. These significant signals last only a few months. The correlation is shown for December when the most statistical correlation is shown in the polar NH before the middle atmospheric CO signal is affected by NH stratospheric sudden warmings, which occurred in January and/or February of 2006, 2009, and 2010 in the mesosphere. Data for one month (December and July, respectively) from CO and TSI/FUV observations over ~8 years have enough samples to show the statistically significant correlations. The sensitivity of CO to the FUV solar-cycle variability is estimated in terms of ppmv per % change of FUV, by regressing the CO VMR on the unit percent change of the FUV irradiance.

We evaluate the statistical significance of the regressed coefficients using a *Student*'s t statistic applied to the correlation coefficient r with n^*–2 degrees of freedom:

$$t = r\sqrt{\frac{n^*-2}{1-r^2}} \tag{4}$$

The effective sample size n^* is estimated using the *Quenouille*'s procedure as described by Angell and Korshover (1981).

The CO response to solar forcing is not homogeneous both horizontally and vertically, especially to the 27-day forcing, because the CO anomalies are transported from one region to another region. To better understand these dynamically–coupled atmospheric responses, we look for the lagged correlation between TSI and MLS CO at different altitudes during the boreal winter when the descent is strongest in the polar middle and upper atmosphere.

The thermospheric and mesospheric CO responds to the 27-day solar forcing with an enhanced VMR through the photolysis at frequencies near the Lyman-α. Most of the radiation at this portion of the solar spectrum does not penetrate down to the mesosphere; therefore there is almost no direct response to it in the mesospheric CO. However, the mesospheric CO may have the 27-day signal resulted from the downward transport of the 27-day solar cycle modulated thermospheric CO. This indirect response occurs only in the winter polar region where the air is descended from the thermosphere and mesosphere (Andrews et al., 1987; Garcia and Boville, 1994).

3. Results and discussions

Aura MLS monthly CO VMR shows a strong interannual variation during the period of 2004–2012 that correlates in phase with the TSI data (Fig. 1). In the NH, the CO at 82°N, 0.005 hPa varies by about 16%, showing less than 22 ppmv in the 2006–2009 as solar irradiance reaches the minimum, and more than 26 ppmv as the TSI increases towards solar maximum after 2009. Similarly, in the SH, CO changes significantly with solar cycle. The solar irradiance variation influence on the photolysis and transport from the low thermosphere likely plays the key role in the interannual variability of wintertime CO distribution.

The observed CO sensitivity to TSI during this period of observation can be used to infer the CO modulation by the solar-cycle in other periods of time, for example for one year since October 1991 when ISAMS (Improved Stratospheric and Mesospheric Sounder) was operating on board the Upper Atmosphere Research Satellite (UARS). The ISAMS instrument provided nearly global coverage with good vertical resolution to examine the CO distribution from 10 hPa to 0.03 hPa. Because the solar activity was at its maximum during 1990–1991, ISAMS took the measurement slightly after the solar maximum (in 1992).

The zonal mean ISAMS CO VMR during the day of January 1992 was ~3.2 ppmv near 60°N at 0.1 hPa (~65 km) (López-Valverde et al., 1996). This amount is slightly higher than the CO measured by Aura MLS at the same height and latitude during December of 2004 and 2011 (~1.8 ppmv and 2.4 ppmv) and January of 2005 and 2011 (~1.4 ppmv and 1.8 ppmv), respectively, since Aura MLS observations do not reach the solar maximum so far. Solar activity was at maximum in 2000 and 2001 with double peaks, and at minimum in 2009 during solar cycle 23. With these caveats the CO value from the ISAMS present a reasonable agreement with the value measured by MLS.

The large vertical gradient in the MLS CO VMR from mesosphere to the low stratosphere (Fig. 2) makes it a good tracer to study the downward transport of CO induced by the solar forcings in the lower thermosphere. The chemical balance between the source and the sink leads to the strong vertical gradient of CO mixing ratios with relatively abundant CO in the upper mesosphere, but with extremely small VMRs in the lower stratosphere. Horizontal CO gradients reflect the transport in the winter polar vortex. The descent in the polar region brings high CO from the mesosphere to the lower stratosphere. The long CO lifetime over 30 days in the polar stratosphere and mesosphere during winter helps to maintain this vertical and horizontal gradients.

The solar cycle signal extends down to the mesosphere and upper stratosphere, as revealed in the correlation coefficient between daily mean MLS CO VMR and daily SORCE TSI for December (Fig. 2(c)) and July (Fig. 2(d)). This extended solar signal is also consistent with the correlation pattern calculated with daily SORCE SOLSTICE FUV irradiance (Fig. 2(e)–(f)). This extended solar signal comes likely from the indirect atmospheric responses to the solar-cycle forcing, as a result of the dynamical transport. However, we did not include any time lag in the correlation analysis in Fig. 2(c)–(f). Therefore, the amplitude of these correlation coefficients may be underestimated. Because the vertical descent is often fast (Lee et al., 2011), the zero lag coefficients can still capture the positive correlation between MLS CO and TSI and they are statistically significant over a wide region from the equator to the winter pole.

Noticeable differences are evident in the downward extension of the solar signal in the December and July correlations. During

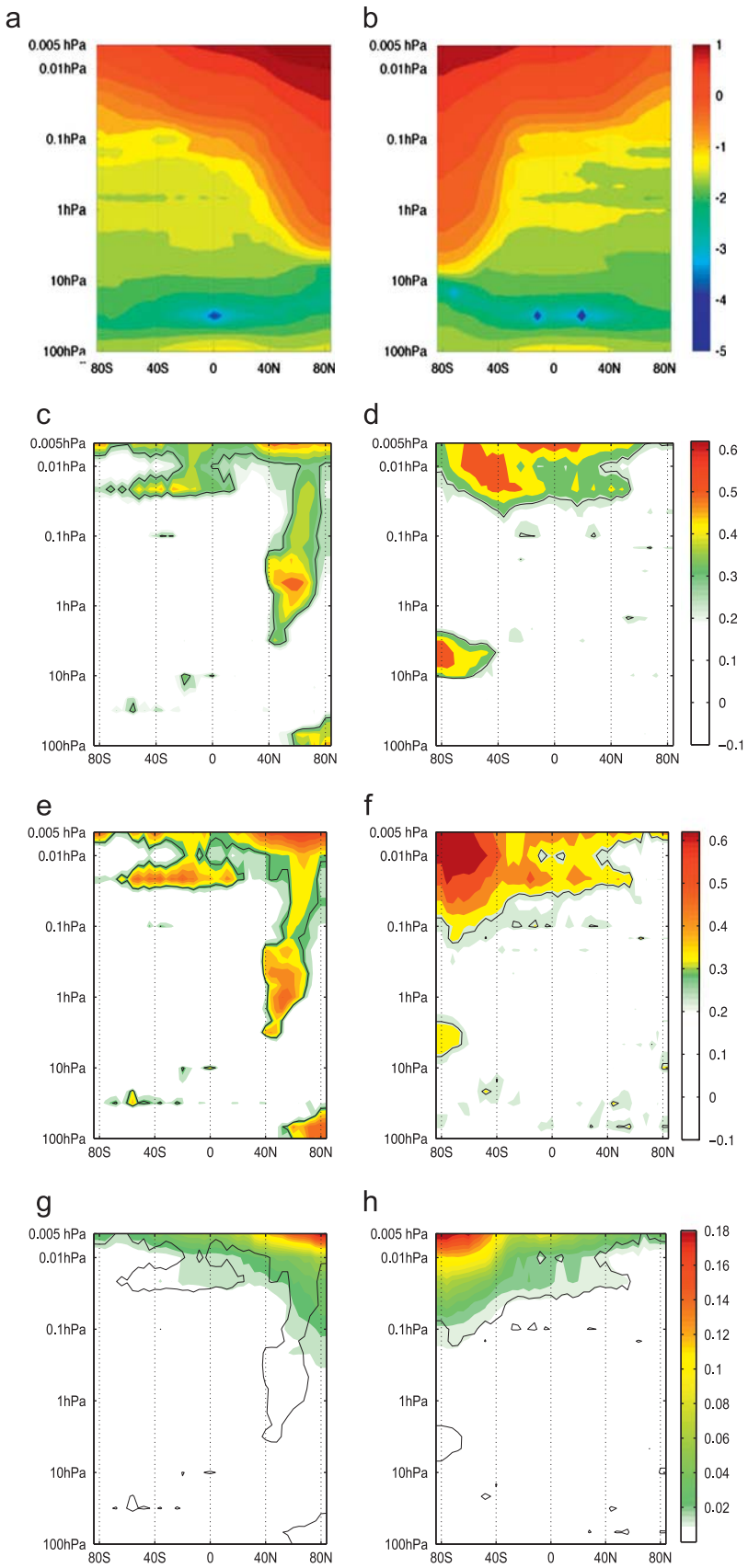

Fig. 2. Daily average of zonal mean MLS CO in Log_{10}(ppmv) as a function of latitude (a) for the December, 2004-2011 (b) for July, 2004–2012. The correlation coefficient between daily SORCE TSI and zonal mean MLS CO VMR calculated for (c) December and (d) July. The correlation coefficient between daily SORCE SOLSTICE FUV and zonal mean MLS CO VMR calculated for (e) December and (f) July. Solid black line bounds the correlations that are different from zero within 95% confidence levels. The sensitivity of CO to the % change of FUV (in ppmv per %) estimated by regressing CO VMR on FUV for (g) December and (h) July. Overlaid line bounds the regression coefficients estimated from the correlations, which are significant within 95% confidence levels.

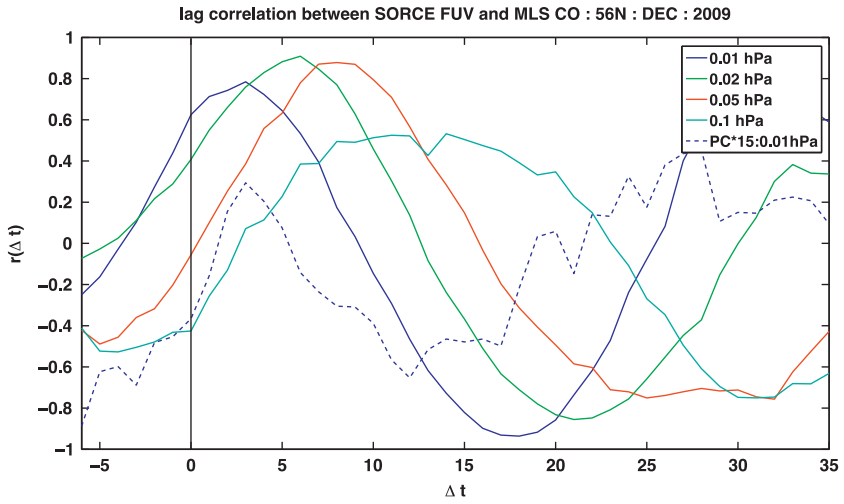

Fig. 3. The time-lag correlation between MLS CO and SORCE FUV during the month of December of 2009 at different altitudes (from 0.1 hPa to 0.01 hPa). Overlaid in blue dash line is the first principal component (PC) of the CO NAM, which accounts for ~30% of the total CO variance from December 2009 to February 2010 in the 20°N–82°N domain.

the boreal winter (December, 2004–2011) (Fig. 2(c) and (e)), the daily correlations between solar irradiance and CO are significant in the winter mesosphere where the CO concentration is high. Strong positive correlation has the largest amplitude in the higher mesosphere (between 0.01 hPa and 0.005 hPa) throughout the equator to the high latitude of winter hemisphere. Those strong signals tend to propagate down to the upper stratosphere (below 1 hPa), due to the wintertime polar descent air from the upper mesosphere when the strong vortex is forming. Similarly, the correlation in the austral winter (July, 2004–2012) shows a strong positive correlation throughout the mesosphere, but the downward extension is weaker in the stratosphere (Fig. 2(d) and (f)). The correlation is more significant more than 0.6 in the SH when the FUV irradiance is used to compute the correlation.

No significant negative correlation between TSI/FUV and CO is found in this analysis, suggesting that an increase in the solar irradiance would cause CO increases in the upper mesosphere and thermosphere. The solar signals are brought downward by dynamics at high latitudes, causing anomalous CO variations in the lower mesosphere and stratosphere. The solar signal in CO is weak in the tropical and summer mesosphere, largely because of lack of vertical transport or horizontal mixing.

We estimate the sensitivity of CO to solar cycle variability by regressing the CO VMR on SORCE FUV (120–160 nm), and show it in ppmv per % change of FUV. As shown in Fig. 2(g)–(h), the maximum CO response to 1% change of FUV can be as high as 0.18 ppmv in the upper mesosphere (~80 km). The sensitivity decreases in the lower mesosphere and stratosphere. Considering the FUV irradiance variance during December of 2004–December of 2009 is over 20% (~2.8×10^{-4} to ~2.3×10^{-4} W/m^2), the change of winter time CO can be as high as ~4 ppmv during the same period. The amplified CO responses indicate that subtle variations in solar irradiance can result in significant atmospheric changes via chemistry and dynamics.

The vertical polar descent causes a delayed CO response to the short-term solar forcing, which can be estimated with the lagged correlation analysis between FUV time series and the CO VMR at different altitudes. In Fig. 3, the lag between the CO and FUV at 56N increases from 3 days in the upper mesosphere (0.01 hPa) to 14 days the upper mesosphere (0.1 hPa). The maximum correlation is decreased below 0.6 at 0.1 hPa. These results suggest that solar signals in CO propagates downward from 0.01 hPa to 0.1 hPa within ~11 days. This descent rate of the solar signal corresponds to ~1.3 km/day and compares well with those estimated from the downward propagation of the maximum CO NAM index (Lee et al., 2011).

This lag between CO and FUV is most noticeable during December of 2009 and 2010 in the Northern Hemisphere, while the event is not obvious in other years and not seen in the Southern Hemisphere. The short term solar signals in CO last only a few months, at most, since CO variability depends on both chemical and dynamical processes. In the mesosphere, the photochemical lifetime of CO (~30 days), is comparable to transport time scales (Solomon et al., 1985) so that solar induced regional CO anomalies may disappear by transport. The short term solar signals in CO are currently in investigation by identifying major patterns of latitude-height variability of CO in the middle atmosphere and details will be discussed in a separate work (Ruzmaikin et al. 2007), to be submitted in *Advances in Space Research*].

To further examine the relation between the solar signal and the middle atmospheric CO anomaly patterns, we computed the principal component (PC) index of the first CO Northern Annular Mode (NAM) during December 2009–February 2010 and compared it with the lagged correlation coefficients. The first EOF mode of geopotential height, called the NAM represents an approximately axially symmetric annular structure of the polar vortex. Similarly, the CO NAM, defined as the first EOF of CO in the middle atmosphere, is axially symmetric annular with a "dome-like" shape centered on the pole, reflecting high CO VMR at the pole and decreasing equatorward. The positive index of CO NAM represents abundant CO mixing ratios in high latitudes, indicating strong descent within the strong vortex. The spatial pattern at different altitude and time–height development of these modes are described in the previous work (Lee et al., 2011). As shown in Fig. 3 (dashed line), the CO NAM index at 0.01 hPa, derived independently from solar variability, has the 27-day variation and is in phase with the lag correlation between FUV and CO at 0.01 hPa.

4. Conclusions

We analyzed MLS CO and SORCE TSI/FUV data to examine the solar influence on the atmospheric CO during the period of 2004 to 2011. Statistically significant positive correlation between MLS CO and TSI/FUV is found in the upper mesosphere. The positive correlation is extended down to the upper stratosphere at the winter high latitudes where the strong polar vortex is present.

Aura MLS monthly averaged CO over 70N during December varies by about 16% over the 11-yr solar cycle. Due to its long photochemical lifetime and strong vertical gradient in the mesosphere, CO acts as a good dynamics tracer to study indirect effects of the upper-atmospheric solar signal and the transport of these anomalies down to the lower atmosphere.

The correlation between MLS CO and the SORCE TSI/FUV is significant (as high as 0.6) in a wide region of upper atmosphere in both hemispheres. The observed positive correlation between FUV and CO suggests that the increased solar irradiance could lead to an abundant CO VMR via the CO_2 photolysis throughout the upper mesosphere due to the deep-penetrating solar UV spectral forcing. The enhanced CO can also be transported to the lower mesosphere and upper stratosphere by dynamics through the vertical diabatic descent in the winter polar vortex, which extends the CO-TSI and CO-FUV correlation to lower altitudes.

We also observed the CO responses to the solar 27-day variation in the polar mesosphere, which progress downward with a time lag from 3 days at 0.01 hPa to 14 days at 0.1 hPa. Because of the long CO photochemical lifetime, the CO solar signal can be transported by the polar descent to lower altitudes, showing lagged responses in CO with height. The mean descent rate, estimated from the lagged CO-TSI correlation, is ~1.3 Km/day, which is consistent with the value derived by Lee et al. (2011).

Because the solar UV spectrum is critical to the CO photolysis, it is not surprising to see a higher correlation with FUV-CO than TSI-CO. Observations of spectral solar irradiance (SSI) are valuable for a more comprehensive understanding of atmospheric responses to solar spectral forcing. The SSI data from SORCE SOLSTICE will be utilized within the full wavelength range of measurement (120–320 nm) if the uncertainty estimates is completed for each wavelength. Updated degradation trend at different wavelength range in the latest SOLSTICE data products will be helpful to estimate more reliable UV variance with solar cycle. Furthermore, a complete solar cycle will be useful to estimate an amplitude of CO and other tracer changes over short term (~27 day) and long term (11 year) solar cycle. Such a reliable long term SSI data is a key in understanding the sun-climate connections, particularly in characterizing which spectral changes of the Sun's radiative output can play a role in different species of the Earth's atmosphere.

Acknowledgments

This work is supported by the NASA Living With a Star Targeted Research and Technology Program (NNH10ZDA001N-LWSTRT). We thank the Aura MLS and SORCE teams for providing their data and analysis support. We thank two anonymous reviewers for valuable comments and suggestions that led to an improved manuscript.

References

Allen, D.R., et al., 1999. Observations of middle atmosphere CO from the UARS ISAMS during the early northern winter 1991/1992. Journal of the Atmospheric Sciences 56, 563–583.

Allen, D.R., Stanford, J.L., Nakamura, N., Lopez-Valverde, M.A., Lopez-Puertas, M., Taylor, F.W., Remedios, J.J., 2000. Antarctic polar descent and planetary wave activity observed in ISAMS CO from April to July 1992. Geophysical Research Letters 27, 665–668.

Angell, J.K., Korshover, J., 1981. Comparison between sea surface temperature in the equatorial eastern Pacific and United States surface temperature. Journal of Applied Meteorology 20, 1105–1110.

Andrews, D.G., Holton, J.R., Leovy, C.B., 1987. Middle Atmospheric Dynamics. Academic Press, New York pp. 1–489.

Brasseur, G.P., Solomon, S., 2005. Aeronomy of the Middle Atmosphere, 3rd ed. Springer, Dordrecht, The Netherlands pp. 1–646.

Filipiak, M.J., Harwood, R.S., Jiang, J.H., Li, Q., Livesey, N.J., Manney, G.L., Read, W.G., Schwartz, M.J., Waters, J.W., Wu, D.L., 2005. Carbon monoxide measured by the EOS microwave limb sounder on Aura: first results. Geophysical Research Letters 32, L14825, http://dx.doi.org/10.1029/2005GL022765.

Garcia, R.R., Boville, B.A., 1994. Downward control of the mean meridional circulation and the temperature of the polar winter stratosphere. Journal of the Atmospheric Sciences 51, 2238–2245.

Harder, J.W., Fontenla, J.M., Pilewskie, P., Richard, E.C., Woods, T.N., 2009. Trends in solar spectral irradiance variability in the visible and infrared. Geophysical Research Letters 36, L07801, http://dx.doi.org/10.1029/2008GL036797.

Haigh, J.D., Winning, A.R., Toumi, R., Harder, J.W., 2010. An influence of solar spectral variations on radiative forcing of climate. Nature 467, 696–699 http://dx.doi.org/10.1038/nature09426,Oct.

Jackman, C.H., et al., 2008. Short- and medium-term atmospheric constituent effects of very large solar proton events. Atmospheric Chemistry and Physics 8, 765–785.

Jackman, C.H., et al., 2009. Long-term middle atmospheric influence of very large solar proton events. Journal of Geophysical Research 114, D11304, http://dx.doi.org/10.1029/2008JD011415.

Jackman, C.H., et al., 2011. Northern hemisphere atmospheric influence of the solar proton events and ground level enhancement in January 2005. Atmospheric Chemistry and Physics 11, 6153–6166, http://dx.doi.org/10.5194/acp-11-6153-2011.

Jin, J.J., Semeniuk, K., Beagley, S.R., Fomichev, V.I., Jonsson, A.I., McConnell, J.C., Urban, J., Murtagh, D., Manney, G.L., Boone, C.D., Bernath, P.F., Walker, K.A., Barret, B., Ricaud, P., Dupuy, E., 2009. Comparison of CMAM simulations of carbon monoxide (CO), nitrous oxide (N_2O), and methane (CH_4) with observations from Odin/SMR, ACE-FTS, and Aura/MLS. Atmospheric Chemistry and Physics 9, 3233–3252.

Kopp, G., Lawrence, G., 2005. The Total Irradiance Monitor (TIM): instrument design. Solar Physics 230, 1–2, http://dx.doi.org/10.1007/s11207-005-7446-4.

Kopp, G., Heuerman, K., Lawrence, G., 2005. The Total Irradiance Monitor (TIM): instrument calibration. Solar Physics 230, 111–127, http://dx.doi.org/10.1007/s11207-005-7447-3.

Kopp, G., Lean, J.L., 2011. A new, lower value of total solar irradiance: evidence and climate significance. Geophysical Research Letters 38, L01706, http://dx.doi.org/10.1029/2010GL045777.

Li, K.F., Jiang, X., Liang, M.-C., Yung, Y.L., 2012. Simulation of solar-cycle response in tropical total column ozone using SORCE irradiance. Atmospheric Chemistry and Physics 12, 1–26, http://dx.doi.org/10.5194/acpd-12-1-2012.

Lee, J.N., Wu, D.L., Manney, G.L., Schwartz, M.J., Lambert, A., Livesey, N.J., Minschwaner, K. R., Pumphrey, H.C., Read, W.G., 2011. Aura Microwave Limb Sounder observations of the polar middle atmosphere: dynamics and transport of CO and H_2O. Journal of Geophysical Research 116, D05110, http://dx.doi.org/10.1029/2010JD014608.

López-Valverde, M.A., López-Puertas, M., Remedios, J.J., Rodgers, C.D., Taylor, F.W., Zipf, E.C., Erdman, P.W., 1996. Validation of measurements of carbon monoxide from the improved stratospheric and mesospheric sounder. Journal of Geophysical Research 101 (D6), 9929–9955, http://dx.doi.org/10.1029/95JD01715.

Marsh, D., 2011. Chemical–Dynamical Coupling in the Mesosphere and Lower Thermosphere, Aeronomy of the Earth's Atmopshere and Ionosphere. Springer, Dordrecht, The Netherlands pp. 1–477.

McClintock, W.E., Rottman, G., Woods, T.N., 2005a. Solar-stellar irradiance comparison experiment II (SOLSTICE II): instrument concept and design. Solar Physics 230, 225.

McClintock, W.E., Snow, M., Woods, T.N., 2005b. Solar-stellar irradiance comparison experiment II (SOLSTICE II): pre-launch and on-orbit calibrations. Solar Physics 230, 259.

Merkel, A.W., Harder, J.W., Marsh, D.R., Smith, A.K., Fontenla, J.M., Woods, T.N., 2011. The impact of solar spectral irradiance variability on middle atmospheric ozone. Geophysical Research Letters 38, L13802, http://dx.doi.org/10.1029/2011GL047561 2011.

Minschwaner, K., et al., 2010. The photochemistry of carbon monoxide in the stratosphere and mesosphere evaluated from observations by the Microwave Limb Sounder on the Aura satellite. Journal of Geophysical Research 115, D13303, http://dx.doi.org/10.1029/2009JD012654.

Parkinson, W.H., Rufus, J., Yoshino, K., 2003. Absolute absorption cross section measurements of CO_2 in the wavelength region 163–20 nm and the temperature dependence. Chemical Physics 290, 251–256.

Pilewskie, P., Rottman, G., Richard, E., 2005. An overview of the disposition of solar radiation in the lower atmosphere: connections to the SORCE snge. Solar Physics 230 (1), 55–69.

Pumphrey, H.C., et al., 2007. Validation of middle-atmosphere carbon monoxide retrievals from the Microwave Limb Sounder on Aura. Journal of Geophysical Research 112, D24S38, http://dx.doi.org/10.1029/2007JD008723.

Rottman, G., 2005. The SORCE Mission. Solar Physics 230 (1), 7–25.

Ruzmaikin, A., Santee, M.L., Schwartz, M.J., Froidevaux, L., Pickett, H., 2007. The 27-day variations in stratospheric ozone and temperature: new MLS data. Geophysical Research Letters 34, L02819, http://dx.doi.org/10.1029/2006GL028419.

Snow, M., McClintock, W.E., Rottman, G., Woods, T.N., 2005. Solar-stellar irradiance comparison experiment II (SOLSTICE II): examination of the solar stellar comparison technique. Solar Physics 230, 295.

Solomon, S., et al., 1985. Photochemistry and transport of carbon monoxide in the middle atmosphere. Journal of the Atmospheric Sciences 42 (1072-1083), 1985.

Swartz, W.H., Stolarski, R.S., Oman, L.D., Fleming, E.L., Jackman, C.H., 2012. Middle atmosphere response to different descriptions of the 11-yr solar cycle in spectral irradiance in a chemistry-climate model. Atmospheric Chemistry and Physics 12, 5937–5948.

Yoshino, K., Esmond, J.R., Sun, Y., Parkinson, W.H., Ito, K., Matsui, T., 1996. Absorption cross section measurements of carbon dioxide in the wavelength region 118.7–175.5 nm and the temperature dependence. Journal of Quantitative Spectroscopy and Radiative Transfer 55, 53.